

LETTERS

Production Rates of Photochemical Reactions by Pulsed Laser Excitation on the Example of the NaHg Molecule

D. Gruber[†]

Institut für Experimentalphysik, Technische Universität Graz, Petersgasse 16, A-8010 Graz

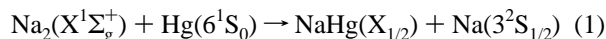
Received: January 3, 1997; In Final Form: May 27, 1997[⊗]

We report on the determination of the reaction rate of photochemical reactions in the gas phase, taking NaHg as an example. The lifetimes as well as the reaction rates are determined by fitting the analytical solution of a simplified set of rate equations to the experimental measured time evolutions of the products of the photochemical reaction. In this way we also extracted the activation energies according to the Arrhenius relation for the NaHg molecule to be produced in their $\text{II}_{1/2}$ and $\text{III}_{1/2}$ electronically excited states, respectively.

I. Introduction

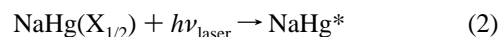
Gas phase photochemistry is important not only for the production of excimers but also for understanding the physics and chemistry of the atmosphere. A crucial point in describing the photochemical reactions properly is the knowledge of the reaction rates. In the present work, using the example of NaHg, we discuss the determination of the reaction rate of a photochemical reaction employing pulsed laser excitation of the reactants.

Although thorough investigations of the NaHg molecule have been published previously (see ref 1 and references therein), not very much is known about the lifetimes of its electronically excited states and the production rates of common photochemical reactions leading to production of such molecules. This for sure is due to the fact that the NaHg molecule has only a very shallow ground state with a dissociation energy of about 430 cm^{-1} . Production of this molecule in the gas phase by a reaction according to



requires typical temperatures of $T = 800 \text{ K}$, which corresponds to a thermal energy of $3kT = 1670 \text{ cm}^{-1}$ and exceeds the

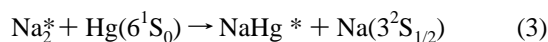
dissociation energy of $\text{NaHg}(\text{X}_{1/2})$ by far. This means that a nascent NaHg molecule would dissociate again on a picosecond scale. Consequently, the equilibrium distribution would be far from any reasonable amount of NaHg in its electronic ground state. Thus application of photochemical production methods is necessary to investigate this molecule by spectroscopic techniques with a high signal to noise ratio. Moreover, a direct access to the lifetimes of electronically excited molecular states of NaHg by an excitation scheme according to



with observation of subsequent fluorescence is possible only with a small signal to noise ratio.

On the other hand, we recently reported on production of the electronically excited $\text{NaHg}(\text{III}_{1/2}, \text{II}_{3/2})$ by a reactive three-body collision following energy-pooling collisions of laser excited $\text{Na}(3^2\text{P})$.¹ Although we investigated the time behavior of the NaHg bands, by the complex kinetics of this processes it was not possible to find the lifetimes of the $\text{NaHg}(\text{III}_{1/2}, \text{II}_{3/2})$ states.

In this work, the common and well-known photochemical reaction



[†] E-mail: icecube@fexphal01.tu-graz.ac.at.

[⊗] Abstract published in *Advance ACS Abstracts*, July 1, 1997.

TABLE 1: Molecular Transitions in Na₂ Induced by the Second and Third Harmonic of the Nd:YAG Laser with the Corresponding Franck–Condon Factors (FCF)

v''	J''	E'', cm^{-1}	v'	J'	E', cm^{-1}	λ, nm	$\Delta\lambda, \text{nm}$	FCF
$X^1\Sigma_g^+ - B^1\Pi_u^a$								
8	76	-3883.82	0	75	14 906.58	532.006	0.0060	2
9	69	-3886.55	1	68	14 903.82	532.007	0.0068	8
9	100	-3164.64	2	99	15 624.98	532.028	0.0281	69
10	73	-3668.00	2	74	15 122.10	532.014	0.0145	24
10	94	-3187.29	3	93	15 603.85	531.985	-0.0150	115
11	58	-3805.24	3	58	14 985.65	531.992	-0.0079	50
11	99	-2925.64	4	100	15 864.72	532.007	0.0071	149
12	54	-3730.57	4	55	15 059.99	532.001	0.0015	85
12	87	-3091.92	5	87	15 698.78	531.997	-0.0025	158
$X^1\Sigma_g^+ - C^1\Pi_u^b$								
8	81	-3773.11	0	80	24 393.34	354.906	0.0062	401
9	44	-4289.33	0	43	23 878.02	354.895	-0.0051	154
9	48	-4236.03	0	48	23 930.55	354.905	0.0046	154
9	52	-4178.33	0	53	23 988.57	354.901	0.006	154
9	82	-3611.24	1	83	24 556.22	354.894	-0.00651	118
10	33	-4269.99	1	32	23 896.37	354.907	0.0074	590

^a FCF from Demtröder *et al.*¹⁶ ^b FCF from Verma *et al.*¹⁷

employing the laser-excited Na₂* molecule as a reactant, which here is in either the B¹Π_u or the C¹Π_u state, is used to produce the NaHg molecule in the II_{1/2} and III_{1/2} states, respectively. The fluorescence spectra as well as the time evolution of the chemiluminescence of the NaHg molecules are investigated. Assisted by a kinetic model of the chemical reaction, for the first time the reaction rates as well as the activation energies for process 3 along with the lifetimes of the electronically excited II_{1/2} and III_{1/2} states of NaHg are determined.

II. Experiment

The experimental setup used throughout these experiments is nearly identical to those reported previously.¹ The Na + Na₂ + Hg vapor mixture is prepared in a stainless steel crossed heat pipe oven terminated by four quartz windows. Argon is used as the buffer gas. A Baratron vacuum gauge is used to determine the buffer gas pressure; the temperature is controlled by a thermocouple device and a current-stabilized power supply. The heat pipe device is operated as described by Gruber *et al.*¹

Laser radiation used to excite the Na₂ molecules is provided by the second and third harmonics of a Q-switched Nd:YAG laser (Quanta Ray GCR 170), respectively. In order to enlarge the reaction volume in the central zone of the heat pipe we omit focusing the laser.

Fluorescence light is focused perpendicular to the excitation laser beam by a quartz lens onto the end of an optical fiber. Spectral resolution is obtained by means of a 50 cm scanning monochromator (Acton) equipped with a holographic grating (1200 grooves/mm). Fluorescence spectra are detected by an optical multichannel analyzing system (OMA). The monochromator is also equipped with a mirror that enables, by rotation through 90°, imaging of the light passing through the monochromator onto an exit slit. Time behavior of fluorescence is detected either by a fast photomultiplier tube (Hamamatsu R-955) with a rise time of 2.2 ns or by a photodiode with an effective rise time of 1 ns mounted on the exit slit and connected to a 600 MHz LeCroy digital storage oscilloscope triggered by the laser controller.

III. Experimental Results

Upon exciting the Na₂ molecule with the second harmonic of the Nd:YAG laser ($\lambda = 532 \text{ nm}$), the Na₂(B¹Π_u) states listed in Table 1 are populated. The laser-induced transitions are

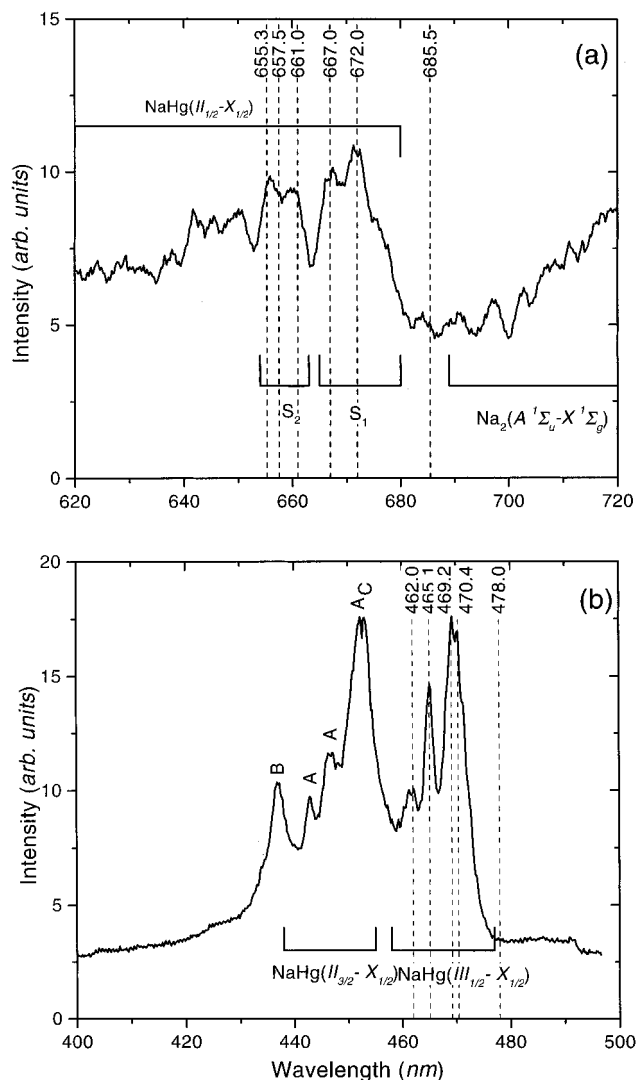
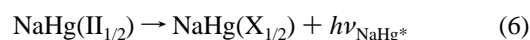
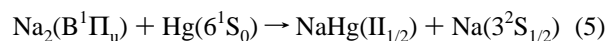
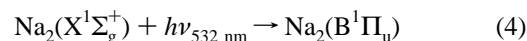
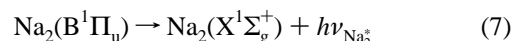


Figure 1. NaHg chemiluminescence following laser excitation of the Na₂ molecule at $T = 790 \text{ K}$, $p = 20 \text{ kPa}$: (a) $\lambda_{\text{laser}} = 532 \text{ nm}$, S₁ and S₂ refer to previously reported NaHg emission bands; (b) $\lambda_{\text{laser}} = 355 \text{ nm}$. (A) NaHg(II_{3/2} - X_{1/2}), (B) Na₂(2³Π_g - 1³Σ_u⁺), (C) Na₂(2¹Σ_u⁺ - X¹Σ_g⁺). The vertical dashed lines indicate the spectral positions of the time measurements.

computed on the basis of the data of Richter *et al.*² and Babaky and Hussein.³ According to the reaction sequence



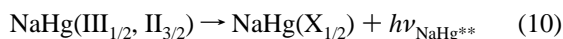
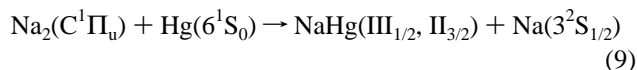
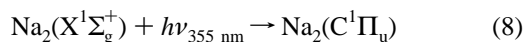
and



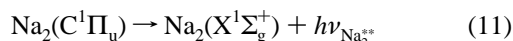
we obtain the spectrum shown in Figure 1a. Besides the NaHg(II_{1/2} - X_{1/2}) red bands in the wavelength range 600–680 nm,⁴ we observe a fraction according to the Na₂(A¹Σ_u⁺ - X¹Σ_g⁺) transition, observable from 690 nm on and extending toward higher wavelengths. The population of the Na₂(A¹Σ_u⁺) state is due to collision-induced radiationless relaxations of the initially populated B¹Π_u state.⁵ For the sake of homogeneity, the indications S₁ and S₂ of the red NaHg bands refer to the assignments in previously published papers.^{4,6,7} The

dashed vertical lines indicate the spectral positions for which time measurements are taken.

The same principles work for the case of excitation of the Na₂ molecule with the third harmonic ($\lambda = 355$ nm) of the Nd:YAG laser. The corresponding transitions listed in Table 1 are computed with the data of Yan *et al.*⁸ The reaction sequence 4–7 then simply is written



and



The relevant fractions of the resulting fluorescence spectra are shown in Figure 4b. As for excitation with the second harmonic, where the originally populated B¹Π_u state relaxes to the A¹Σ_g⁺ state, in this case the C¹Π_u state also decays by collision-induced radiationless relaxations to the 2¹Σ_g⁺ and to the 2³Π_g states (see B and C in Figure 1b). The well-known bands corresponding to the Na₂(2¹Σ_g⁺ – X¹Σ_g⁺) and Na₂(2³Π_g – 1³Σ_g⁺) transitions⁹ lie in the same wavelength range as the NaHg(II_{3/2} – X_{1/2}) bands and thus exclude these bands from being investigated in this work.

According to the properties of a heat pipe oven,¹⁰ we regard the particle density n to be given by the relation

$$n_i = \frac{p_i(T)}{kT} \quad (12)$$

where T is the temperature of the oven, $p_i(T)$ is the partial pressure of the considered species, and k is the Boltzmann constant. In a real heat pipe mode, the metal inside the heated zone evaporates at a temperature given by the buffer gas pressure p . But, if p exceeds the vapor pressure of the metal for a certain temperature, the particle density n is given by the vapor pressure corresponding to the temperature T . Thus, in order to investigate the dependance of the time behavior of the NaHg fluorescence on Na₂ particle density, we varied the temperature of the heat pipe oven.

The lifetime measurements are taken for the wavelengths shown in Figure 1. For the reasons discussed above, it is not possible to investigate the time behavior of the NaHg(II_{3/2} – X_{1/2}) bands. In order to account for the background due to Na₂ fluorescence, we also measure the time evolution at 685.5 and 478.0 nm. This spectral positions are known to be free of any NaHg fluorescence, since the NaHg red bands terminate at about 670 nm and the blue bands at about 475 nm.^{4,1} The background time curves then simply are subtracted from the NaHg signal. It is found that all time evolutions of the red II_{1/2} – X_{1/2} bands differ only marginally among each other as do the results for the blue III_{1/2} – X_{1/2} bands. Thus in Figure 2 we only present representative results for $\lambda_{\text{NaHg}^{**}} = 672.0$ nm (a) and $\lambda_{\text{NaHg}^{**}} = 496.2$ nm (b). The time scales of the evolutions in Figure 2 are shifted numerically, so that the exciting laser pulse has its maximum at the time $t = 0$ ns. It clearly can be seen that after the laser pulse the signals of the NaHg fluorescence approach

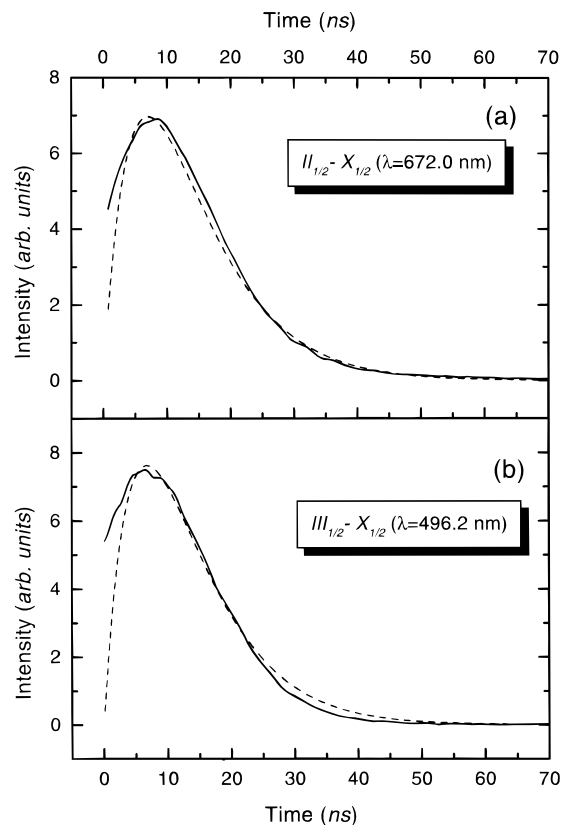


Figure 2. Representative time evolutions of the fluorescence signals of the NaHg red (a) and blue bands (b), for the same experimental parameters as in Figure 1. The dashed lines represent the results of the numerical treatment.

their peak intensities with a delay of about $\tau_{\text{delay}} = 10$ ns and then decay monotonically.

IV. Analysis and Discussions

As shown in eqs 5 and 9, the NaHg molecules are produced from Na₂ molecules, which initially are populated by the excitation laser pulse. From this it is obvious that the fluorescence of the NaHg molecules can only appear with a certain time delay that is connected to the decay times of the reactant's electronically excited states, i.e. Na₂(B¹Π_u) and Na₂(C¹Π_u), as well as to the reaction rates k_1 and k_2 of processes 5 and 9.

In order find an analytical solution to this problem that can be fitted to the experimental results, we have to use a simple kinetic model employing the following set of rate equations

$$\frac{dn_{\text{Na}_2(i)}(t)}{dt} = -(A_{\text{Na}_2(i)}n_{\text{Na}_2(i)}(t) - (k_{\text{NaHg}(i)}n_{\text{Na}_2(i)}(t)n_{\text{Hg}}) \quad (13)$$

$$\frac{dn_{\text{NaHg}(i)}(t)}{dt} = -(A_{\text{NaHg}(i)}n_{\text{NaHg}(i)}(t) - (k_{\text{NaHg}(i)}n_{\text{Na}_2(i)}(t)n_{\text{Hg}}) \quad (14)$$

where the index i refers to the different sets of electronically excited states of the Na₂ and the NaHg molecules according to

λ_{laser}	Na ₂ (i)	NaHg(i)
532 nm	B ¹ Π _u	II _{1/2}
355 nm	C ¹ Π _u	III _{1/2}

In order to obtain an analytical solution of eqs 13 and 14, we

neglect stimulated emission processes as well as radiation trapping effects. This seems to be reasonable, since the particle density of the Na₂ molecules is low enough so that the impact of these effects should not influence the results. In the case of the Na₂ molecule, the reactants' states are B¹Π_u and C¹Π_u, whereas the products' states are II_{1/2} and III_{1/2}, depending on whether the vapor mixture is excited by the second or the third harmonic of the Nd:YAG laser. The rate constant $k_{\text{NaHg}(i)}$ refers to the photochemical production, where the index i is II_{1/2} for eq 5 and III_{1/2} for eq 9. According to the Arrhenius equation¹¹ we write the rate constant as

$$k_{\text{NaHg}(i)} = A_{(i)} e^{-\epsilon_{A(i)}/kT} \quad (15)$$

where $\epsilon_{A(i)}$ is the activation energy of reactions 5 and 9 and $A_{(i)}$ is the respective preexponential factor. In this way, we can also account for the temperature dependence of the rate constant $k_{\text{NaHg}(i)}$.

The time evolution of the system is calculated, starting at the time when the excitation laser pulse has its maximum. For the sake of simplicity of the solutions, we treat the laser pulse as an infinite perturbation of the system. That offers the advantage that the solution of the rate equations remains analytical, but we lose the representation of the time evolution in the first few nanoseconds, namely during the time when the laser intensity is decaying toward zero. The second and third harmonics of the Nd:YAG laser saturate the transitions listed in Table 1. Accounting for the Boltzmann vibrational population distribution in the electronic ground state, the population of the excited states easily can be calculated.

Consequently, for the Na₂ molecules we regard the initial condition

$$n_{\text{Na}_2(i,v'')}(0) = \frac{n_{\text{Na}_2(v'')}}{2} \quad (16)$$

to be valid throughout the experiments, where $n_{\text{Na}_2(v'')}$ stands for the total number density of Na₂ molecules in a specific vibrational state v'' . For the NaHg molecule we set

$$n_{\text{NaHg}(i)}(0) = 0 \quad (17)$$

With the initial conditions 16 and 17, the solution of the rate equations 13 and 14 is

$$n_{\text{Na}_2(i)}(t) = \frac{1}{2} n_{\text{Na}_2} e^{-(k_{\text{NaHg}(i)} n_{\text{Hg}} + A_{\text{Na}_2(i)})t} \quad (18)$$

$$n_{\text{NaHg}(i)}(t) = \frac{1}{2} \frac{k_{\text{NaHg}(i)} n_{\text{Na}_2} n_{\text{Hg}}}{k_{\text{NaHg}(i)} n_{\text{Hg}} + A_{\text{Na}_2(i)} - A_{\text{NaHg}(i)}} (e^{-A_{\text{NaHg}(i)}t} - e^{-(k_{\text{NaHg}(i)} n_{\text{Hg}} + A_{\text{Na}_2(i)})t}) \quad (19)$$

Employing the vapor pressure tables of Vargaftik *et al.*¹² for Na and Na₂ and those of ref 13 for Hg, we are able to determine the particle densities n_{Na_2} and n_{Hg} for each set of heat pipe temperature and buffer gas pressure. Since the particle density of Hg always is about 3 orders of magnitude larger than those of Na₂, we regard it to be constant in time.¹ The effective Einstein coefficients $A_{\text{Na}_2(i)}$ for the B¹Π_u and C¹Π_u states including lifetime shortening by collisions are taken from the experiment, so that the only variables in eq 19 are $k_{\text{NaHg}(i)}$ and $A_{\text{NaHg}(i)}$.

The fit of eq 19 to the experimental results also includes a factor that accounts for the scaling of the time evolutions that is kept constant for all time behaviors investigated. Representative results of the fitting procedure are shown in Figure 2 by

TABLE 2: Numerical Results for the Einstein Coefficients A_{NaHg} of the II_{1/2} and III_{1/2} States of NaHg and the Rate Constants k_{NaHg} for Reactions 5 and 9^a

T, K	$A_{\text{NaHg}}, 10^8 \text{ s}^{-1}$	$\Delta A_{\text{NaHg}}, 10^8 \text{ s}^{-1}$	$k_{\text{NaHg}}, 10^{-18} \text{ m}^3 \text{ s}^{-1}$
NaHg(II _{1/2})			
749.0	0.97	0.02	4.7
762.0	0.97	0.02	4.9
778.0	1.00	0.02	5.4
791.0	1.01	0.02	5.7
799.5	1.03	0.02	5.8
816.0	1.07	0.02	6.4
820.0	1.09	0.02	6.8
836.0	1.14	0.02	7.2
842.0	1.14	0.02	7.1
NaHg(III _{1/2})			
760.0	1.27	0.09	30.0
779.0	1.47	0.07	32.0
789.0	1.66	0.12	33.8
816.0	1.93	0.13	37.4
827.2	2.18	0.29	40.6
840.6	2.66	0.13	42.8
849.0	2.84	0.36	45.3
852.8	3.01	0.15	44.7

^a The error ΔA_{NaHg} is due to the averaging of the results for the single wavelengths. The error of the Einstein coefficients as well as the rate constants is found to be less than 10%.

the dashed lines. The deviation of the model from the experimental results for $t < 5$ ns is due to the treatment of the laser pulses discussed above. The origin of the time axis is shifted to coincide with the second half value of the peak intensity of the laser pulse, appearing about 2 ns after the peak, thus leading to production of NaHg even before the virtual origin of the time scale of the model. Anyway, this circumstance has no impact on the results.

Since, as discussed previously, the time curves of the red as well as blue bands differ only marginally for the various wavelengths (Figure 1), we average the fitting parameters to get $k_{\text{NaHg(II}_{1/2})}$ and $A_{\text{NaHg(II}_{1/2})}$ corresponding to the red bands and $k_{\text{NaHg(III}_{1/2})}$ and $A_{\text{NaHg(III}_{1/2})}$ corresponding to the blue bands. The numerical results are presented in Table 2. Figure 3 shows a graphical representation according to the Stern–Vollmer¹⁴ relation

$$A_{\text{eff}} = A_{\text{rad}} + n\sigma\bar{u} = A_{\text{rad}} + \sigma_{\text{coll}} \sqrt{\frac{8}{\pi\mu kT}} p \quad (20)$$

where $A_{\text{eff}} = 1/\tau_{\text{eff}}$ is connected to the effective lifetime and $A_{\text{rad}} = 1/\tau_{\text{rad}}$ to the radiative lifetime, σ_{coll} is the cross section for collisional deactivation, n is the particle density obeying relation 12, and \bar{u} is the mean relative velocity ($\bar{u} = (8kT/\pi\mu)^{1/2}$) of the collision partners with the reduced mass $1/\mu = \sum_i 1/m_i$. The slope of the linear fit describes the coefficient $\sigma(8/\pi\mu k)^{1/2}$ in eq 20 and thus is connected to the cross section for collisional deactivation σ . Qualitatively it can be seen that the slope for the III_{1/2} – X_{1/2} transitions is much larger than for the red II_{1/2} – X_{1/2} bands. We ascribe this to the fact that in the vicinity of the III_{1/2} state there lie several other electronic states that might serve as the final state of collisional quenching processes and thus decrease the lifetime drastically if the number of potential collision partners, i.e., Na and Na₂, is increased. Especially the Na₂ molecule, although present only in a small fraction, with its large geometrical diameter has to be considered as an important collision partner for these quenching processes.

In order to find the activation energies $\epsilon_{A(i)}$ we fit the experimental results of $k_{\text{NaHg}(i)}$ to eq 15, with the preexponential

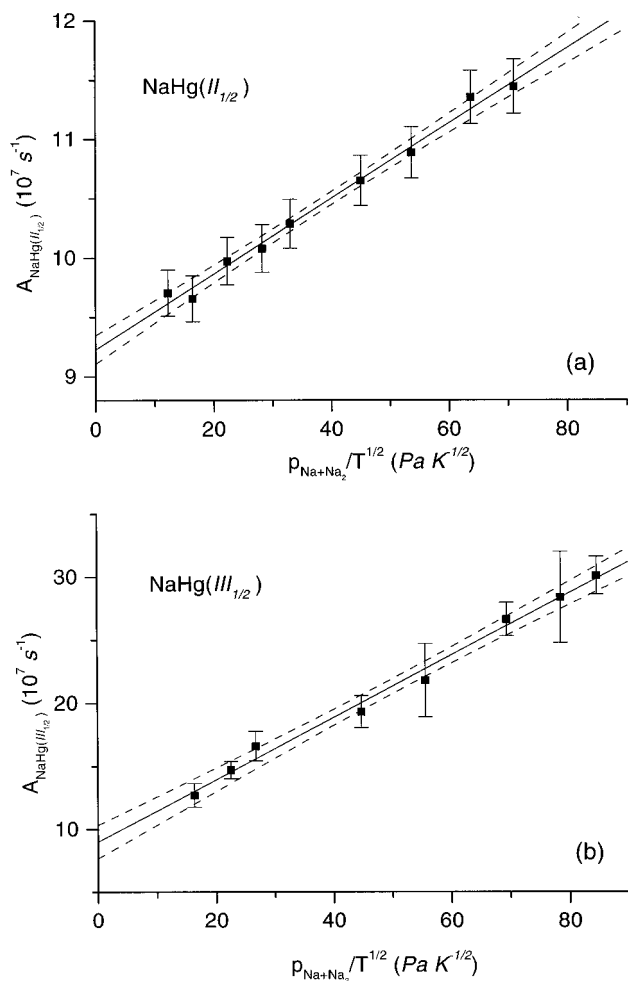


Figure 3. Einstein coefficients A of (a) the $\text{II}_{1/2}$ and (b) the $\text{III}_{1/2}$ states of NaHg depending on the total sodium pressure $p_{\text{Na}+\text{Na}_2}$ divided by the square root of the temperature T . The solid lines show the results of a fit according to eq 20; the dashed lines indicate the 95% confidence bands.

factor written as

$$A_{(i)} = \sigma \cdot \bar{u} = \sqrt{\frac{8kT}{\mu\pi}} \sigma \quad (21)$$

where σ is the cross section for reactions 5 and 9. The results along with the statistical errors of $k_{\text{NaHg}(i)}$ are shown in Figure 4, and the numerical values are listed in Table 3.

We find the activation energies to be of the same order of magnitude as determined for a similar reaction of Na_2 with $\text{Cd}(5^1\text{S}_0)$ that has been published previously.¹⁵ It also can be seen that the rate of reaction 9 is larger than the result for eq 5. This difference might be explained by the longer lifetime of the reactant's state, i.e., $\text{C}^1\Pi_u$, compared to the $\text{B}^1\Pi_u$ state in reaction 5. Consequently the probability of the laser-excited Na_2 molecule to collide with a ground state Hg and to produce a NaHg molecule is larger for eq 9. This also can be seen directly from a comparison of the reaction rates in Figure 4.

V. Conclusion

We determined the reaction rates for photochemical reactions producing excimers in the gas phase at high temperatures. Therefore, we developed a simplified kinetic model of the chemical reactions occurring in our experiment, which is capable of being solved analytically. On the basis of the experimentally measured time evolutions of both the product NaHg and the

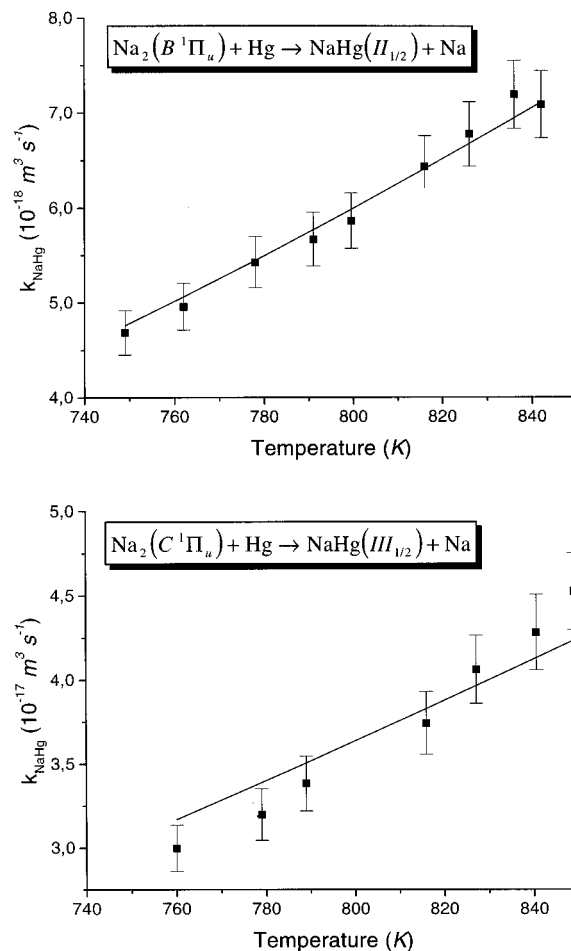


Figure 4. Reaction rates $k_{\text{NaHg}(\text{II}_{1/2})}$ and $k_{\text{NaHg}(\text{III}_{1/2})}$ for the reactions 5 and 9, respectively, depending on temperature T . The solid line represents the results of the numerical fit according to eq 15.

TABLE 3: Results for the Activation Energies ϵ_A and Reaction Cross Sections σ for Reactions 5 and 9 for the $\text{II}_{1/2}$ and $\text{III}_{1/2}$ States S of NaHg

S	ϵ_A , cm^{-1}	σ , nm^2
$\text{II}_{1/2}$	1600 ± 400	0.3 ± 0.1
$\text{III}_{1/2}$	1200 ± 600	0.6 ± 0.2

Na_2 reactants concentrations following pulse laser preparation of the Na_2 electronically excited states, the extraction of the rate constants and activation energy was possible.

The method presented seems to be a useful tool to determine reaction rates of laser induced photochemical reactions. Especially for reactions that involve products with a short lived electronic ground state, such as excimers or radicals, the complications in analyzing the product concentration can be overcome by applying this method.

In subsequent experiment, the investigation of reaction rates of chemical reactions involving the OH radical are planned.

Acknowledgment. I would like to thank Prof. H. Jäger and Prof. L. Windholz for permanent scientific support and critical discussions. I also thank A. Seifert and N. Koch for supporting work in the laboratory. This work was financially supported by the Fonds zur Förderung der Wissenschaftlichen Forschung, project no. P-9929-PHY, by the Jubiläumsfonds der Österreichischen Nationalbank, project no. 4873, and by the European Scientific Foundation in the framework of the REHE programs (relativistic effects in heavy-element chemistry and physics).

References and Notes

- (1) Gruber, D.; Domiaty, U.; Iskra, K.; Dinev, S.; Windholz, L. *J. Phys. Chem.* **1996**, *100*, 7078.
- (2) Richter, H.; Knöckel, H.; Tiemann, E. *Chem. Phys.* **1991**, *157*, 217.
- (3) Babaky, O.; Hussein, K. *Can. J. Phys.* **1988**, *67*, 912.
- (4) Gruber, D.; Domiaty, U.; Li, X.; Windholz, L.; Gleichmann, M. M.; Hess, B. A. *J. Chem. Phys.* **1995**, *102*, 5174.
- (5) Hussein, K.; Aubert-Frécon, M.; Babaky, O.; D'Incan, J.; Effantin, C.; Vergés, J. *J. Mol. Spectrosc.* **1985**, *114*, 105.
- (6) Schlejen, J.; Woerdmann, J. P.; Pichler, G. *J. Mol. Spectrosc.* **1988**, *128*, 1.
- (7) Windholz, L.; Zerza, G.; Pichler, G.; Hess, B. A. *Z. Phys. D: At. Mol. Clusters* **1991**, *18*, 373.
- (8) Yan, G.-Y.; Sterling, B. W.; Kalka, T.; Schawlow, A. L. *J. Opt. Soc. Am. B* **1989**, *6*, 1975.
- (9) Pichler, G.; Bahns, J. T.; Sando, K. M.; Stwalley, W. C.; Konowalow, D. D.; Li, L.; Field, R. W.; Müller, W. *Chem. Phys. Lett.* **1986**, *129*, 425.
- (10) Vidal, C. R.; Cooper, J. *J. Appl. Phys.* **1969**, *40*, 3370.
- (11) Wayne, R. P. Theory of Kinetics. In *Comprehensive Chemical Kinetics*; Bamford, C. H., Tipper, C. F. H., Eds.; Elsevier: Amsterdam, 1969; Vol. II, p 189.
- (12) Vargaftik, N. B.; Voljak, L. D. In *Handbook of Thermodynamic and Transport Properties of Alkali Metals*; Ohse, R. W., Ed.; Blackwell Scientific Publications: Oxford, 1985.
- (13) Weast, R. C., Astle, M. J., Ed. *CRC Handbook of Chemistry and Physics*; CRC Press: Boca Raton, FL, 1982.
- (14) Demtröder, W. *Laser Spectroscopy*, 2nd ed.; Springer: Berlin, Heidelberg, 1996.
- (15) Gruber, D.; Domiaty, U.; Windholz, L.; Jäger, H.; Musso, M.; Allegrini, M.; Fuso, F.; Winkler, A. *J. Chem. Phys.* **1994**, *100*, 8103.
- (16) Demtröder, W.; Stetzenbach, W.; Stock, M.; Witt, J. *J. Mol. Spectrosc.* **1976**, *61*, 382.
- (17) Verma, K. K.; Vu, T. H.; Stwalley, W. C. *J. Mol. Spectrosc.* **1982**, *91*, 325.